

# Experimental implementation of high-fidelity unconventional geometric quantum gates using NMR interferometer

Jiangfeng Du,<sup>1,2,\*</sup> Ping Zou,<sup>1</sup> and Z. D. Wang<sup>3,†</sup>

<sup>1</sup>*Hefei National Laboratory for Physical Sciences at Microscale & Department of Modern Physics, University of Science and Technology of China, Hefei, Anhui 230026, China*

<sup>2</sup>*Department of Physics, National University of Singapore, 2 Science Drive 3, Singapore 117542*

<sup>3</sup>*Department of Physics & Center of Theoretical and Computational Physics, University of Hong Kong, Pokfulam Road, Hong Kong, China*

(Dated: February 1, 2008)

Following a key idea of unconventional geometric quantum computation developed earlier [Phys. Rev. Lett. 91, 197902 (2003)], here we propose a more general scheme in such an intriguing way:  $\gamma_d = \alpha_g + \eta\gamma_g$ , where  $\gamma_d$  and  $\gamma_g$  are respectively the dynamic and geometric phases accumulated in the quantum gate operation, with  $\eta$  as a constant and  $\alpha_g$  being dependent only on the geometric feature of the operation. More arrestingly, we demonstrate the first experiment to implement a universal set of such kind of generalized unconventional geometric quantum gates with high fidelity in an NMR system.

PACS numbers: 03.67.Lx, 03.65.Vf, 76.60.-k

Quantum computation has been paid intensive interest for the past decade because quantum computers are believed to be much more powerful and efficient than their classical counterparts due to their quantum nature[1]. Significant progresses have recently been achieved in the field of quantum computing. Nevertheless, there are still great challenges in physical implementation of quantum computation. One of them is to suppress the noises in quantum gates to an acceptable level, which is essential to build a scalable quantum computer. Recently, a promising approach based on geometric phases[2, 3, 4] was proposed to achieve built-in fault-tolerant quantum gates with higher fidelities[5, 6, 7, 8, 9, 10, 11] since the geometric phase depends only on the global feature of the evolution path and is believed to be robust against local fluctuations. On the other hand, in the same spirit, an interesting unconventional geometric quantum computation(GQC) scheme was proposed[12]; such kind of two-qubit gate was indeed reported experimentally in trapped ions[13] and was designed with superconducting qubits[14]. In this scheme, the dynamic phase  $\gamma_d$  is ensured to be proportional to the geometric phase  $\gamma_g$ , namely,  $\gamma_d = \eta\gamma_g$ , ( $\eta \neq 0, -1$ ) with  $\eta$  as a proportional constant.

In this paper, we propose that the above unconventional GQC scheme[12] can be further generalized in such an intriguing manner:  $\gamma_d = \alpha_g + \eta\gamma_g$ , where  $\alpha_g$  is a coefficient dependent only on the geometric feature of the quantum evolution path in the gate operation. It is elaborated that this generalized unconventional GQC can be realized in physical systems like NMR. In particular, we report the first experimental implementation of a universal set of such kind of unconventional geometric gates with high fidelity in an NMR system.

Before we present our new results, let us first elucidate how to realize a single-qubit gate with the general-

ized unconventional geometric phase shift in the cyclic evolution[11]. For an one-qubit system, consider two orthogonal cyclic states  $|\psi_+\rangle$  and  $|\psi_-\rangle$ , which satisfy the relation  $U(\tau)|\psi_\pm\rangle = \exp(\pm i\gamma)|\psi_\pm\rangle$ , where  $\gamma$  is the total phase accumulated and  $U(\tau)$  is the evolution operator of a cyclic evolution with  $\tau$  as the periodicity. We can write  $|\psi_+\rangle = e^{-i\frac{\phi}{2}} \cos \frac{\chi}{2} |\uparrow\rangle + e^{i\frac{\phi}{2}} \sin \frac{\chi}{2} |\downarrow\rangle$  and  $|\psi_-\rangle = -e^{-i\frac{\phi}{2}} \sin \frac{\chi}{2} |\uparrow\rangle + e^{i\frac{\phi}{2}} \cos \frac{\chi}{2} |\downarrow\rangle$ , where  $(\chi, \phi)$  are the spherical coordinates of the state vector on the Bloch sphere (Fig.1),  $|\uparrow\rangle$  and  $|\downarrow\rangle$  are the two eigenstates of the  $z$ -component of the spin-1/2 operator ( $\sigma_z/2$ ) and they constitute the computational basis for the qubit. For an arbitrary input state denoted as  $|\psi_{in}\rangle = a_+|\psi_+\rangle + a_-|\psi_-\rangle$  with  $a_\pm = \langle\psi_\pm|\psi_{in}\rangle$ , after the cyclic evolution for the  $|\psi_+\rangle$  ( $|\psi_-\rangle$ ) state, the output state is  $|\psi_{out}\rangle = U(\gamma, \chi, \phi)|\psi_{in}\rangle$ , where

$$U = \begin{pmatrix} e^{i\gamma} \cos^2 \frac{\chi}{2} + e^{-i\gamma} \sin^2 \frac{\chi}{2} & ie^{-i\phi} \sin \gamma \sin \chi \\ ie^{i\phi} \sin \gamma \sin \chi & e^{i\gamma} \sin^2 \frac{\chi}{2} + e^{-i\gamma} \cos^2 \frac{\chi}{2} \end{pmatrix}. \quad (1)$$

In the same spirit as that in Ref. [12], once we are able to ensure that the total phase  $\gamma$  is a generalized unconventional geometric phase given by

$$\gamma = \alpha_g + (1 + \eta)\gamma_g, \quad (2)$$

this  $U$ -gate is an unconventional geometric quantum gate. For example, along a cyclic evolution path  $A-B-N-A$  on the Bloch sphere in Fig.1, it is found that  $\gamma_d = -\pi/2 - \gamma_g$ , and thus the unconventional geometric phase ( $-\pi/2$ ) will be accumulated in the qubit-state. The corresponding  $U$ -gate is just an unconventional GQC gate. In the experiment, the two single-qubit gates to be chosen are  $U_1 = \begin{pmatrix} -i & 0 \\ 0 & i \end{pmatrix}$ , ( $\gamma = -\pi/2, \chi = 0$ ,  $\phi = 0$ ) and  $U_2 = -i/\sqrt{2} \begin{pmatrix} 1 & 1 \\ 1 & -1 \end{pmatrix}$ , ( $\gamma = -\pi/2, \chi = \pi/4$ ,

$\phi = 0$ ). As is well known, to achieve a set of universal quantum gates, in addition to the above two noncommutative single-qubit gates, we need also to construct one nontrivial two-qubit gate based on unconventional geometric phase shifts. In the present work, a nontrivial two-qubit gate is obtained when the loop is controlled by another qubit; for example the controlled loop  $N$ - $A$ - $B$ - $N$  leads to a controlled unconventional GQC gate:

$$U_c = \begin{pmatrix} -i & 0 & 0 & 0 \\ 0 & i & 0 & 0 \\ 0 & 0 & 1 & 0 \\ 0 & 0 & 0 & 1 \end{pmatrix} \quad (3)$$

We now demonstrate how to achieve the above unconventional GQC gates using NMR interferometer, noting that the NMR has been a mature technology to simply illustrate certain quantum information processing methods in recent years and a number of important experiments like the demonstration of the Shor algorithm have been reported[15]. In our NMR experiment, the two-qubit NMR system is 0.5ml, 20mmol sample of carbon-13 labelled chloroform ( $\text{CHCl}_3$ ) dissolved in  $\text{d}_6$  acetone [16]. Qubit  $a$  is identified as the carbon-13 nucleus and qubit  $b$  as the hydrogen. The Hamiltonian of the system is written as:

$$H = \omega_a I_z^a + \omega_b I_z^b + 2\pi J I_z^a I_z^b, \quad (4)$$

where the first two terms characterize the free procession of spin carbon-13 and hydrogen about the externally applied, strong static  $B_0$  with frequencies  $\omega_a/2\pi \simeq 100\text{MHz}$  and  $\omega_b/2\pi \simeq 400\text{MHz}$ , and  $I_z^a$  and  $I_z^b$  are the  $z$  components of the angular momentum operators for

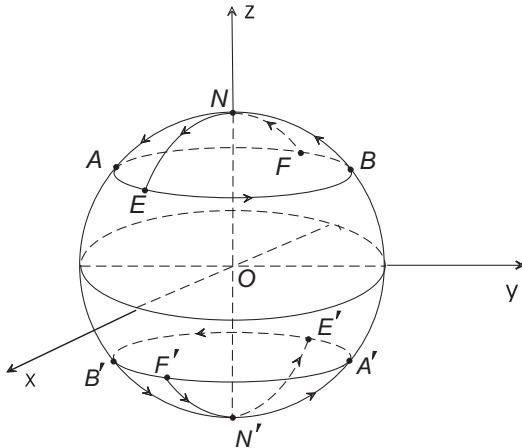


FIG. 1: The cyclic paths in the experiments. When  $|\psi_+\rangle$  loops along the path  $N$ - $A$ - $B$ - $N$ , and  $|\psi_-\rangle$  loops along path  $N'$ - $A'$ - $B'$ - $N'$ , the phases gained are  $-\pi/2$  and  $\pi/2$ , correspondingly. The polar angle of  $A$  is arbitrary between 0 and  $\pi/2$ .

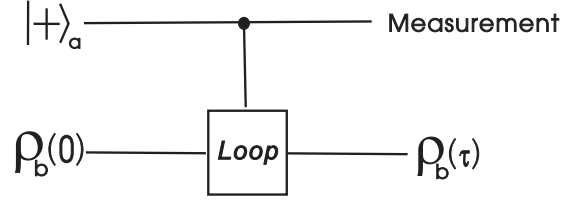


FIG. 2: The quantum network to measure the unconventional geometrical phase, which is in fact a two-qubit gate. The top horizontal line represents an auxiliary spin half particle, or an auxiliary qubit, labeled as qubit  $a$ . The bottom line represents a qubit labeled as  $b$ , in state  $\rho_b$  which undergoes a cyclic evolution induced by a unitary operation  $U(\tau)$ . We choose our reference basis, for qubits  $a$  and  $b$ , to be states  $|\uparrow\rangle$  and  $|\downarrow\rangle$ . In this basis  $|\pm\rangle = 1/\sqrt{2}(|\uparrow\rangle \pm |\downarrow\rangle)$ , thus the initial state of auxiliary qubit is  $|\uparrow\rangle_a$ . The phase gained by qubit  $b$  after the evolution operation  $U(\tau)$  is detected by a phase sensitive detector.

qubit  $a$  and qubit  $b$  ( $I_z^a = 1/2\sigma_z^a$ ,  $I_z^b = 1/2\sigma_z^b$ ). The third term characterizes a scalar spin-spin coupling of the two spins with  $J = 214.5\text{Hz}$ . The spin-spin relaxation time are 0.35s for carbon and 3.3s for proton, respectively.

Initially the two qubits are in thermal equilibrium with the environment and their state is described by the density operator  $\rho_{th} \propto I_z^a + 4I_z^b$ . We use the "spatial averaging" technique to prepare the effective pure state  $|00\rangle$ , or in the density operator form:  $\frac{1}{2}(1+2I_z^a) \otimes \frac{1}{2}(1+2I_z^b)$ . The NMR pulse sequence to generate this state is:  $R_x^b(\frac{\pi}{3}) - G_z - R_x^b(\frac{\pi}{4}) - \frac{1}{2J} - R_{-y}^b(\frac{\pi}{4}) - G_z$ , where  $R_x^b(\alpha) = e^{-i\alpha I_x}$  denotes a hard pulse applied on qubit  $b$  to make it rotate around the  $x$  axis by angle  $\alpha$  ( $R_{-x}^b(\alpha) = R_x^b(-\alpha)$ ).  $G_z$  indicates a  $z$ -gradient which destroys all coherences ( $x$  and  $y$  magnetizations) and retains only longitudinal magnetization ( $z$  magnetization component), and  $\frac{1}{2J}$  represents a time interval during which only the third term of the Hamiltonian evolves.

In the beginning, we measure the unconventional geometric phase when the state evolves along the loop we have designed. The quantum network utilized and a brief measurement description are presented in Fig.2. Qubit  $a$  is the auxiliary qubit to help observe the phase of qubit  $b$  acquired when undergoing a cyclic evolution path in Fig.1. The Hamiltonian for spin  $b$  in rotational framework of rotation speed  $\omega'_b = \omega_b - \pi J$  is given by

$$H_b = (\omega_b - \omega'_b \pm \pi J) I_z^b \quad (5)$$

Note here that  $H_b$  is dependent on the state of qubit  $a$  through the term  $\pm J$ . Explicitly, it is  $2\pi J I_z^b$  if the state of qubit  $a$  is  $|\psi_a\rangle = |\uparrow\rangle$ , and it is zero if the state of qubit  $a$  is  $|\psi_a\rangle = |\downarrow\rangle$ .

The NMR RF pulse sequence can be expressed as

$$R_y^b(-\frac{\pi}{2}) - \tau_1 - R_y^b(\frac{\pi}{2}) - \tau_2 - R_y^b(-\frac{\pi}{2}) - \tau_1 - R_y^b(\frac{\pi}{2}). \quad (6)$$

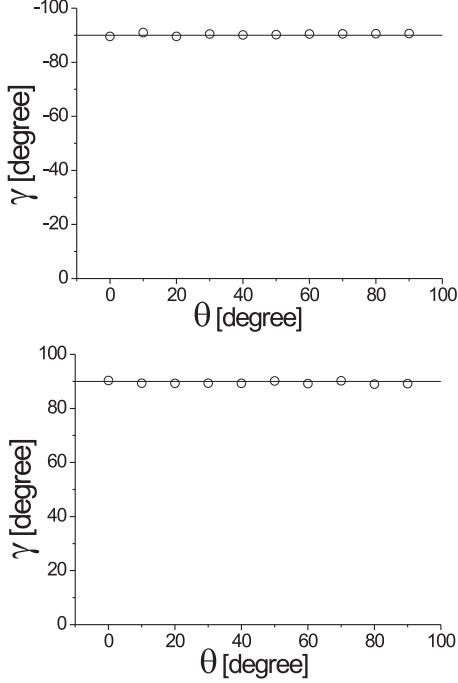


FIG. 3: The measured unconventional geometric phases in our NMR experiment. The two reference states evolve respectively along the path  $N$ - $A$ - $B$ - $N$  (up) and  $N'$ - $A'$ - $B'$ - $N'$  (down) [see Fig.1]. We set the polar angle  $\theta$  of  $A$  to be  $n\pi/18$  ( $n = 0, 1, 2, \dots, 9$ ) and  $m\pi/18$  ( $m = 9, 10, 11, \dots, 18$ ) for  $A'$ . The measured results are in excellent agreement with Eq.(2) with  $\alpha_g = -\pi/2$  and  $\eta = -1$ .

We interpret the process in detail as follows. Supposing that the starting point is  $N$ , rotating firstly qubit  $b$  around the axis  $y$  with the angle  $\frac{\pi}{2}$  transforms the Hamiltonian of qubit  $b$  to  $2\pi JI_x^b$  if it is not zero. This operation is denoted by  $R_y^b(-\frac{\pi}{2})$ . Note that  $|\omega_b - \omega_a|$  is much larger than  $J$ , hence the state of qubit  $a$  is (almost) unaffected by any operation on qubit  $b$  in the whole process. The interaction Hamiltonian will create an evolution path on the geodesic curve  $N$ - $A$  during the interval  $\tau_1 = \frac{\theta}{2J}$ . The next step is to rotate qubit  $b$  around the  $y$  axis with  $\frac{\pi}{2}$  to let the Hamiltonian return to the original one. During the interval  $\tau_2 = \frac{\pi}{2J}$ , the state evolves freely through the path  $A$ - $B$ . Then repeat the same operations as mentioned above  $R_y^2(\frac{\pi}{2}) - \tau_1 - R_y^2(\frac{\pi}{2})$ , qubit  $b$  will return to the starting point with a phase  $\gamma$  being accumulated. While the phase is zero when qubit  $a$  is  $|\psi_a\rangle = |\downarrow\rangle$ . As a results, the auxiliary qubit acquires an internal phase factor  $e^{i\gamma}$ , i.e.,  $1/\sqrt{2}(|\uparrow\rangle + |\downarrow\rangle) \mapsto 1/\sqrt{2}(e^{i\gamma}|\uparrow\rangle + |\downarrow\rangle)$ . Exploiting a phase sensitive detector on qubit  $a$ , we can observe/determine this phase  $\gamma$ .

In the experiment, the rotation operations on qubit  $b$  were performed by hard pulses. The phases accumulated via the two designated paths:  $N$ - $A$ - $B$ - $N$  and  $N'$ - $A'$ - $B'$ -

$N'$  were measured. In the loop  $N$ - $A$ - $B$ - $N$ , the polar angle of  $A$  is set as  $\theta = n\pi/18$  ( $n = 0, 1, 2, \dots, 9$ ), and in the loop  $N'$ - $A'$ - $B'$ - $N'$ , the polar angle of  $A'$  as  $\theta = m\pi/18$  ( $m = 9, 10, 11, \dots, 18$ ). The results are depicted in Fig.3, which are in excellent agreement with Eq.(2) (with  $\alpha_g = -\pi/2$  and  $\eta = -1$ ). Therefore, this evolution loop can be used to construct the set of unconventional geometrical phase gates  $U_1$ ,  $U_2$ , and  $U_c$ , which will be demonstrated in the experiment detailed below. In addition, we adopt the averaged gate fidelity, defined as

$$\mathcal{F} = \overline{\langle \Psi_{in} | \hat{U}^\dagger \rho_{out} \hat{U} | \Psi_{in} \rangle}, \quad (7)$$

to measure the precision of the experimentally implemented gates with respect to an ideal one, where the over-line denotes the average over all possible input states  $|\Psi_{in}\rangle$ , and  $\hat{U}$  is the unitary operator corresponding to the ideal gate.

In our experiment, two single-qubit gates were implemented by performing the following procedures. In consideration of the symmetry of the two qubits, both gates were implemented on spin (qubit)  $a$ , with spin (qubit)  $b$  being decoupled by spin echoes. In both processes to realize the single-qubit gates, the irradiation frequency of the carbon channel was set as  $\varpi_a - 4\pi J$  and  $\varpi_b$  for the hydrogen channel, so the Hamiltonian in this rotating frame reads  $H_a = 4\pi JI_z^a$ .

(i) By applying the NMR pulse sequence  $R_x^a(\frac{\pi}{4}) - \frac{1}{8J} - R_x^b(\pi) - \frac{1}{8J} - R_{-x}^b(\pi) - R_x^a(\frac{\pi}{4})$ , in which the  $\pi$  pulses on spin  $b$  are used to cancel the coupling  $J$  of the two qubits. Under the pulse sequence the starting state  $|0\rangle$  cycles along path  $N$ - $A$ - $B$ - $N$  with the state  $|1\rangle$  being meanwhile along the path  $N'$ - $A'$ - $B'$ - $N'$ . Since  $\gamma = -\pi/2, \chi = \phi = 0$ , we achieve the gate operation  $U_1$  from Eq.(1). The average fidelity of one qubit gate may be evaluated by simply averaging the fidelities of six axial pure states on the Bloch Sphere [18]:  $|0\rangle, |1\rangle, |0\rangle \pm |1\rangle, |0\rangle \pm i|1\rangle$ . In the experiment, by quantum state tomography, the fidelities of the six pure states were measured as 0.999, 0.999, 0.982, 0.990, 0.969 and 0.983, thus the average fidelity is 0.985.

(ii) By applying another NMR pulse sequence  $\frac{1}{8J} - R_x^2(\pi) - \frac{1}{8J} - R_{-x}^2(\pi) - R_y^a(\frac{\pi}{2})$ , the state  $|\psi_+\rangle = \cos\frac{\pi}{8}|\uparrow\rangle + \sin\frac{\pi}{8}|\downarrow\rangle$  cycles along the path  $E$ - $F$ - $N$ - $E$  while  $|\psi_-\rangle = \sin\frac{\pi}{8}|\uparrow\rangle - \cos\frac{\pi}{8}|\downarrow\rangle$  along the mirror loop  $E'$ - $F'$ - $N'$ - $E'$  on south hemisphere. As a result, the logic gate  $U_2$  is realized, with the fidelity 0.975.

(iii) We now turn to address how to realize a non-trivial two-qubit gate experimentally. Figure 2 shows a schematic network of a two-qubit gate. If qubit  $a$  is in the state  $|\uparrow\rangle$ , an evolution path of  $N$ - $A$ - $B$ - $N$  (or  $N'$ - $A'$ - $B'$ - $N'$ ) on the Bloch sphere is produced for qubit  $b$ ; if qubit  $a$  is in the state  $|\downarrow\rangle$ , nothing happens to qubit  $b$ . This is equivalent to say that the time evolution operator satisfies the relation:  $U(\tau)|\psi_\pm\rangle = e^{\mp i\pi/2}|\psi_\pm\rangle$  if qubit  $a$  is up, while  $U(\tau) = 1$  if qubit  $a$  is down. Here  $|\psi_\pm\rangle$  correspond to point  $N$  and  $N'$  respectively in the Bloch sphere,

with  $\mp\pi/2$  are the unconventional geometrical phases acquired respectively. Therefore the two-qubit logical gate  $U_c$  is obtained.

This is a nontrivial conditional phase gate (two-qubit) [8, 11]. To completely characterize the process, we performed a process tomography on the two qubit gate. Using the method described in Ref. [17], we realized quantum state tomography of the 16 states:  $|\psi_k\rangle|\psi_l\rangle$  ( $k, l = 1, \dots, 4$ ), where  $|\psi_1\rangle = |0\rangle$ ,  $|\psi_2\rangle = |1\rangle$ ,  $|\psi_3\rangle = \frac{1}{\sqrt{2}}(|0\rangle + |1\rangle)$ ,  $|\psi_4\rangle = \frac{1}{\sqrt{2}}(|0\rangle + i|1\rangle)$ . The average fidelity of the gate was found to be 0.934, which is higher than that of the conventional dynamical gate.

All our measurements are conducted at room temperature and normal pressure on a Bruker AV-400 spectrometer, and quite high fidelities of a universal set of quantum gates are achieved in NMR systems. Essentially this is due to the fact that such kind of gates are realized by using unconventional geometric phase to fight against decoherence. Therefore, the measured fidelities are robust. However, there are some observed small deviations. Such residual imperfections will always remain in the experiment and may come from imperfect pulses, quantum tomography and inhomogeneity of magnetic field.

In conclusion, we have generalized the idea of unconventional geometric phase gates. It has been illustrated that this generalized unconventional GQC can be implemented in NMR systems. Indeed, we carried out the first experiment to achieve a universal set of such kind of gates with quite high fidelity in NMR systems. Our scheme using the generalized unconventional geometric phase is very interesting and valuable in physical implementation of geometric quantum computation because it can shorten the gate-operation time while keeping the high fidelity. The present scheme may also be feasible in other physical systems, which would stimulate significant experimental interests.

We are grateful to Mianlai Zhou and S. L. Zhu for helpful discussions. This work was supported by the National Fundamental Research Program (Grant No. 2001CB309300), ASTAR under Grant No. R-144-000-071-305, NSFC under Grant Nos. 10425524 & 10429401, the RGC grant of Hong Kong under Nos. HKU7114/02P

&HKU7045/05P, and the URC fund of HKU.

---

\* Electronic address: djf@ustc.edu.cn

† Electronic address: zwang@hkucc.hku.hk

- [1] P. W. Shor, SIAM Rev. **41**, 303(1999).
- [2] M. V. Berry, Proc. R. Soc. London, Ser. A **392**, 45(1984).
- [3] Y. Aharonov and J. Anandan, Phys. Rev. Lett. **58**, 1593 (1987).
- [4] S. L. Zhu, Z. D. Wang, and Y. D. Zhang, Phys. Rev. B **61**, 1142 (2000); S. L. Zhu and Z. D. Wang, Phys. Rev. Lett. **85**, 1076 (2000).
- [5] P. Zanardi and M. Rasetti, Phys. Lett. A **264**, 94 (1999).
- [6] G. Falci, R. Fazio, G. M. Palma, J. Siewert, and V. Vedral, Nature (London) **407**, 355(2000).
- [7] L. M. Duan, J. I. Cirac, and P. Zoller, Science **292**, 1695(2001).
- [8] J. A. Jones, V. Vedral, A. Ekert, and G. Castagnoli, Nature (London) **403**, 869(2000).
- [9] X. B. Wang and M. Keiji, Phys. Rev. Lett. **87**, 097901 (2001).
- [10] S. L. Zhu and Z. D. Wang, Phys. Rev. Lett. **89**, 097902(2002); Phys. Rev. A **66**, 042322 (2002).
- [11] S. L. Zhu and Z. D. Wang, Phys. Rev. A **67**, 022319(2003); X. D. Zhang, S. L. Zhu, L. Hu, and Z. D. Wang, Phys. Rev. A **71**, 014302 (2005).
- [12] S. L. Zhu and Z. D. Wang, Phys. Rev. Lett. **91**, 197902 (2003).
- [13] D. Leibfried, B. DeMarco, V. Meyer, D. Lucas, M. Barrett, J. Britton, W. M. Itano, B. Jelenkovic, C. Langer, T. Rosenband, and D. J. Wineland, Nature (London) **422**, 412 (2003).
- [14] S. L. Zhu, Z. D. Wang, and P. Zanardi, Phys. Rev. Lett. **94**, 100502 (2005).
- [15] L. M. K. Vandersypen and I. L. Chuang, Rev. Mod. Phys. **76**, 1037 (2004).
- [16] J. F. Du, P. Zou, M. Shi, L. C. Kwek, J. -W. Pan, C. H. Oh, A. Ekert, D. K. L. Oi, and M. Ericsson, Phys. Rev. Lett. **91**, 100403(2003).
- [17] J. F. Poyatos and J. I. Cirac, Phys. Rev. Lett. **78**, 390(1997).
- [18] Jae-Seung Lee, Phys. Lett. A **305**, 349 (2002); M. D. Bowdrey, D. K. L. Oi, A. J. Short, K. Banaszak, and J. A. Jones, Phys. Lett. A **294**, 258 (2002).